Imaging parameters of high grade gliomas in relation to the MGMT promoter methylation status: the CT, diffusion tensor imaging, and perfusion MR imaging

Won-Jin Moon · Jin Woo Choi · Hong Gee Roh · So Dug Lim · Young-Cho Koh

Abstract

Introduction We hypothesized that methyl-guanine methyl transferase (MGMT) promoter methylation status, a predictor of the chemosensitivity for high grade gliomas (HGGs), may be associated with computed tomography (CT)/magnetic resonance (MR) imaging variables.

Methods Out of 38 consecutive patients with HGGs, 24 patients whose MGMT promoter methylation status was available [12 men and 12 women; median age, 49 years; age range, 22–79 years; WHO grade III ($n=7$), WHO grade IV ($n=17$)] were enrolled retrospectively. CT attenuation, apparent diffusion coefficient (ADC), fractional anisotropy (FA), and relative cerebral blood volume (rCBV) were measured for enhancing tumors. Qualitative imaging features were also analyzed. Mann–Whitney and Fisher's exact tests were used to evaluate relationships between MGMT promoter methylation status and imaging variables.

Results Maximum CT attenuation was significantly lower in the methylated MGMT promoter group than that in the unmethylated MGMT promoter group (30.3 ± 9.5 HU versus 39.2 ± 4.7 HU, respectively, $p=0.009$). While ADC values tended to be higher in the methylated group than in the unmethylated group ($p=0.055$), ADC ratio was significantly higher, and the FA and FA ratios were significantly lower in the methylated group than in the unmethylated group ($p=0.032$, $p=0.006$ and $p=0.007$, respectively). In contrast, rCBV ratio did not differ between the two groups ($p=0.380$).

Regarding imaging features, only ill-defined margin was seen more frequently in the methylated group than in the unmethylated group (45.5% versus 7.7%, respectively, $p=0.048$).

Conclusion Preoperative imaging can predict MGMT promoter methylation status, which is of paramount importance for predicting treatment response to chemotherapy with an alkylating agent.

Keywords Glioblastoma · Anaplastic gliomas · Chemotherapy · Magnetic resonance imaging (MRI) · Computed tomography (CT)

W.-J. Moon (✉) · J. W. Choi · H. G. Roh
Department of Radiology,
Konkuk University School of Medicine,
4-12, Hwayang-dong, Gwanjin-gu,
Seoul 143-792, South Korea
e-mail: mdmoonwj@naver.com

W.-J. Moon
e-mail: mdmoonwj@kuh.ac.kr

S. D. Lim
Department of Pathology,
Konkuk University School of Medicine,
Seoul, South Korea

Y.-C. Koh
Department of Neurosurgery,
Konkuk University School of Medicine,
Seoul, South Korea

Introduction

High grade gliomas (HGGs), such as WHO grade III (anaplastic glioma, AG) and IV (glioblastoma multiforme, GBM), are rapidly progressive forms of primary brain tumors, and these tumors have an increasing incidence because of the aging population. The prognosis of HGGs has been much improved due to the development of new chemotherapy using a DNA alkylating agent called temozolamide (TMZ) [1]. Nevertheless, the overall median

survival is only 14.6 months for patients with GBM and 2–5 years for patients with AG even with combined therapy of surgical resection, radiotherapy, and TMZ [1, 2].

Recent molecular investigations have revealed that the methylation status of the methyl-guanine methyl transferase (MGMT) gene promoter is associated with a favorable prognosis and prolonged survival for patients with HGGs treated with TMZ [1, 3, 4]. The MGMT promoter gene is located on chromosomal band 10q26. Methylation of the MGMT promoter gene induces low levels of MGMT proteins, which is an ubiquitous DNA repair enzyme, at the cell level. This low level of MGMT proteins induces DNA damage and eventually cell death [5, 6]. Accordingly, a HGG becomes more sensitive to chemotherapy by methylation of the MGMT promoter at the cellular level. The prevalence of MGMT promoter methylation reportedly ranges from 30% to 53% in GBM [7, 8] and from 50% to 84% in AG [4, 9]. Although MGMT promoter methylation is known to be an important prognostic indicator for the outcome of patients with HGGs and a good predictor of the response to alkylating chemotherapy [3, 7, 10], the methylation status of MGMT promoter can only be determined by examining the surgical or biopsy specimen. Moreover, the heterogeneity of HGGs makes unguided surgical biopsy prone to sampling error, resulting in incomplete inclusion of the target area and undergrading in up to 30% of the cases [11, 12]. In the same manner, the methylation status of MGMT promoter can be erroneously determined. Therefore, it would be helpful for the prognostication and predicting the chemoresponse of HGGs to alkylating agents if the MGMT promoter methylation status can be determined noninvasively by preoperative imaging.

Computed tomography (CT), diffusion tensor imaging (DTI) and T2*-dynamic susceptibility weighted contrast enhanced (DSC) perfusion-weighted imaging (PWI) have been extensively studied for their clinical usefulness to predict the grade of glioma or distinguishing recurrent brain tumors from radiation necrosis [13–15]. However, to the best of our knowledge, there have been only two reports on the relationship between the MGMT promoter methylation status and the CT/MR images [16, 17]. The previous reports focused on the imaging texture and tumor location rather than on quantitative imaging parameters such as the diffusion tensor parameters or the perfusion parameters.

We hypothesized that the MGMT promoter methylation status is associated not only with the imaging features as seen in MRI but also with the quantitative imaging parameters, which include the CT attenuation, the apparent diffusion coefficient (ADC) and fractional anisotropy (FA) from DTI, and the regional cerebral blood volume (CBV) from PWI. The purpose of this study was to retrospectively evaluate the relationship between the MGMT methylation status and the quantitative imaging parameters of CT/MR in HGGs.

Materials and methods

This retrospective study was approved by the institutional review board and informed consent was waived.

Patients

Thirty-eight consecutive patients with newly diagnosed histopathologically proven HGGs (WHO grade III or IV, including anaplastic astrocytomas, anaplastic oligodendrogliomas, anaplastic oligoastrocytomas, and GBM) were recruited between August 2006 and June 2009 at our institution. All the pathologies of the HGGs in the 38 patients were examined by an experienced neuropathologist. Among these patients, we considered those for inclusion who had undergone both unenhanced CT and conventional magnetic resonance (MR) imaging with DTI and PWI before surgery or surgical biopsy. Thus, four patients were excluded due to the lack of initial unenhanced CT images, and two patients were excluded due to the lack of DTI. Among the remaining 32 patients with HGGs, 24 patients who underwent evaluation of the methylation status of MGMT promoter in their tumor specimens were finally included in this study. All the HGGs of these 24 patients were confirmed at the time of partial resection ($n=2$), subtotal resection ($n=11$), near total resection ($n=4$), or gross total resection ($n=7$). Standard treatment protocol included radiation therapy plus continuous daily TMZ (75 mg m^{-2} day) followed by six cycles of adjuvant TMZ (150 mg/m^2 for 5 days every 28 days) after surgical resection or surgical biopsy. An overall survival (OS) for each patient was measured from the time of initial diagnosis to death or date of last follow-up.

CT imaging

All the CT scans were obtained with a helical CT scanner (LightSpeed Pro16, GE Medical Systems, Milwaukee, WI, USA). The scanning parameters for unenhanced CT were 120 kVp and 330 mAs with an image matrix of 512×512, a 23- or 24-cm field of view and a 5-mm section thickness.

MR imaging

A 3.0-T unit (Signa HDxt, GE Medical System, Milwaukee, WI, USA) with an eight-channel head coil was used for the MR imaging. The MR imaging protocol included the following conventional sequences: (1) the axial T1-weighted inversion recovery sequences [repetition time (TR)/echo time (TE)/inversion time (TI), 2,468/12/920 ms; field of view (FOV), 220 mm; section thickness (ST)/intersection gap (IG), 5/2 mm; matrix, 512×224], (2) the axial T2-weighted fast spin-echo sequence (TR/effective TE, 4,000/106 ms; FOV, 220 mm; ST/IG, 5/2 mm, matrix: 384×384), (3) the axial

fluid-attenuated inversion recovery sequence (FLAIR; TR/TE/TI, 11,000/105/2,600 ms; FOV, 220 mm; ST/IG, 5/2 mm; matrix, 384×224), (4) the axial T2*-weighted gradient-echo sequence (TR/TE, 550/17 ms; FOV, 220 mm; ST/IG, 5/2 mm; matrix, 384×224; flip angle (FA), 17°.

DTI was obtained by applying six different directions of orthogonal diffusion gradients and b value of 1,000 (TR/TE, 10,000/92.4 ms; FOV, 240 mm; ST/IG, 3.5/0 mm; matrix, 256×256).

Axial T2* DSC-PWI was performed during the administration of gadobutrol (Gadovist; Schering, Berlin, Germany; 0.1 mmol/kg of body weight) with an injection rate of 3 ml/s followed by a saline flush of 20 cc, using the single-shot gradient-echo echo-planar imaging sequence (TR/TE, 1,000/18.9 ms; FOV, 240 mm; ST/IG, 7/0 mm; matrix, 256×256; FA, 60°). Immediately after the acquisition of the DSC-PWI, the post contrast-enhanced 3D fast spoiled gradient-recalled acquisition in the steady state (FSPGR), T1-weighted sequence was obtained (TR/TE, 6.2/2.6 ms; FOV, 220 mm; ST/IG, 1/0 mm; matrix, 512×512).

Quantitative imaging analysis

The CT and MR imaging analyses for the 24 patients were performed in a blinded manner by one experienced neuroradiologist using commercially available software (Functool; GE Medical Systems) on a commercially available imaging processing workstation (Advantage; GE Medical System, Milwaukee, WI, USA). All the MR imaging data that included the postcontrast 3D FSPGR T1-weighted images, the diffusion tensor raw data set, and the perfusion raw data set were transferred to the imaging processing workstation. The T2* DSC-PWI images were used to produce relative CBV (rCBV) maps by using commercially available software (Functool). The rCBV was calculated by integrating the negative enhancement portion of the T2* signal intensity time curve, which is derived from the perfusion data set. The DTI raw data were used to produce the FA and ADC maps using the same software. The postcontrast T1-weighted images were aligned with the rCBV map, the ADC map, and the FA map, as well as the T2-weighted images and the FLAIR images.

To exclude regions with necrosis, hemorrhage, or typical vasogenic edema, we cross-checked the unenhanced T2-weighted and postcontrast T1-weighted MR images. In each patient with tumor, six regions of interest (the size was at least over 20 mm^2) were measured at the enhancing solid portion of the tumors. We selected the lowest minimum ADC value, the lowest minimum FA value, and the highest maximum rCBV value from among these six values for statistical analysis. The ADC, FA, and rCBV ratios were expressed as ratios relative to those in a region of interest of the same size in the contralateral homologous normal-appearing brain parenchyma.

The CT attenuation at the solid portion of the tumors was also measured. When determining the CT attenuation of these lesions, the regions with necrosis, hemorrhage, or typical vasogenic edema were excluded by examining the T2-weighted and postcontrast T1-weighted MR images. Coregistration of the CT and MR images was not performed for analysis. However, the rater carefully compared each pair of CT and MR images to minimize possible errors due to differences in the section position and scan angle based on reference to anatomic landmarks. Six regions of interest (with a size at least over 20 mm^2) were measured at the solid portion of the tumors. We utilized the highest maximum CT attenuation from among those measurements for the statistical analysis.

Qualitative imaging analysis

The CT and MR images were viewed on a standard picture archiving and communication system, and they were assessed independently by two neuroradiologists with 12 years of experience and 5 years of experience, respectively, for the following imaging features: enhancing tumor margin (well defined versus ill defined), tumor enhancement (ring enhancement versus nodular enhancement), the presence of a cystic portion, and the heterogeneity of the signal intensity on the T2-weighted images. When there is a disagreement, conclusion was reached by consensus. Independent assessment results by two reviewers were used to calculate interobserver agreement.

Statistical analysis

Statistical analysis was performed with using commercially available soft ware (PASW Statistics version 17.0; SPSS, Chicago, IL, USA). Because of the small sample size, we used non-parametric statistical analysis.

A median overall survival (OS) was calculated using the Kaplan–Meier method. The log rank test was used to compare the OS according to the MGMT promoter methylation status. The Mann–Whitney test was used to evaluate the relationship between the MGMT promoter methylation and the CT/MR imaging parameters (CT attenuation, ADC, FA, ADC ratio, FA ratio, and rCBV ratio).

The imaging features were visually assessed and correlated with the MGMT promoter methylation status using Fisher's exact test. Interobserver agreement for the imaging feature analysis was calculated using the k statistic, with $k<0.2$, 0.2–0.4, 0.4–0.6, 0.6–0.8, and 0.8–1.0 representing poor, fair, moderate, good, and excellent agreement, respectively [18]. Differences were considered significant for $p<0.05$.

Results

Patient population

Table 1 summarizes the clinicopathological features of the patient population included in this study according to the methylation status of the MGMT promoter. There was no significant difference in gender, age, and the WHO grade and proliferative index such as Ki-67 between the methylated group and the unmethylated group of the HGGs. A median OS of 486 days was observed in all patients with HGGs (95% CI, 371–600 days). A median OS tended to be longer in the methylated group than in the unmethylated group but not with statistical significance (778 and 448 days, respectively, $p=0.164$; Fig. 1).

Difference of the CT attenuation according to the MGMT promoter methylation status

The maximum CT attenuation was significantly lower in the methylated HGGs compared to that in the unmethylated HGGs (30.3±9.5 HU versus 39.2±4.7 HU, respectively, $p=0.009$; Fig. 2a).

Difference of the DTI and PWI parameters

Table 2 summarizes the DTI and PWI measurements between the methylated and unmethylated groups of HGGs. While the ADC values tended to be higher in the methylated HGGs than in the unmethylated HGGs ($p=0.055$), the ADC ratio was significantly higher in the methylated tumors versus the unmethylated tumors ($p=0.032$; Fig. 2b). The FA and FA ratio showed significantly lower values in the methylated HGGs as compared with those in the unmethylated HGGs ($p=0.006$ and $p=0.007$, respectively; Fig. 2c).

In contrast to the DTI parameters, the rCBV ratio did not reveal a significant difference between the methylated group and the unmethylated group ($p=0.380$; Fig. 2d).

Difference of the imaging features

Table 3 summarizes the imaging features that were visually assessed between the two groups of HGGs. An ill-defined enhancing tumor margin was seen more frequently in the methylated HGGs than in the unmethylated HGGs (45.5% versus 7.7%, respectively, $p=0.048$, Fisher's exact test; Figs. 3 and 4). In contrast, ring enhancement, the presence of a cyst, and the heterogeneity of the T2 signal intensity did not differ between the two groups.

Interobserver agreement for an ill-defined enhancing tumor margin, ring enhancement, the presence of a cyst, and the T2 signal heterogeneity was excellent ($k=0.803$, 0.934, 1.000, and 0.872, respectively).

Discussion

We found that the methylation status of the MGMT promoter in HGG is not associated with the rCBV ratio, but it is associated with the CT attenuation and the diffusion tensor parameters such as the ADC and FA. The HGGs with a methylated MGMT promoter were likely to have an ill-defined margin, and they revealed a lower CT attenuation, a higher ADC, and a lower FA.

When alkylating agents, such as TMZ, are introduced in the brain, O^6-methylguanine-DNA-methyltransferase (MGMT), which is a cellular DNA-repair enzyme, is known to remove alkyl groups from the O^6 position of guanine and to inhibit the double-strand DNA cross-linking. Elevated MGMT activity is frequently observed in brain tumors. MGMT itself may cause resistance to alkylating agents in HGGs by allowing DNA repair of tumor cells, and this resistance is directly related to the MGMT content of HGGs [19]. On the other hand, the methylation of the MGMT promoter of HGGs causes decreased activity of MGMT and accordingly inhibits repair of DNA damage following concomitant chemotherapy and radiation therapy [1, 3, 7, 9], which results in prolonged disease-free survival. Given that, our results suggest that HGGs with lower CT attenuation, higher ADC and lower FA values can predict longer survival and greater sensitivity to chemotherapy with TMZ, due to the increased likelihood of having MGMT promoter methylation, than the HGGs with higher CT attenuation, lower ADC, and higher FA values.

Prior to the era of MR imaging, CT has been a major pre-treatment imaging modality for diagnosing glioma. In our study, we observed a negative association between CT attenuation and the methylation status of the MGMT

| **Table 1** Clinicopathological characteristics		No methylation ($n=13$)	Methylation ($n=11$)	p value
OS Overall survival in days	Gender (F/M)	6:7	6:5	0.50
[a] Data are median with range in parentheses	Age (years)	53 (25–73)[a]	49 (27–79)	0.82
	WHO grade (III/IV)	3:10	4:7	0.395
[b] The numbers in parentheses were used to present 95% confidence interval	Ki-67 index (%)	20 (1–60)	8.5 (3–70)	0.483
	Median OS[b]	448 (151–745)	778 (424–1131)	0.164
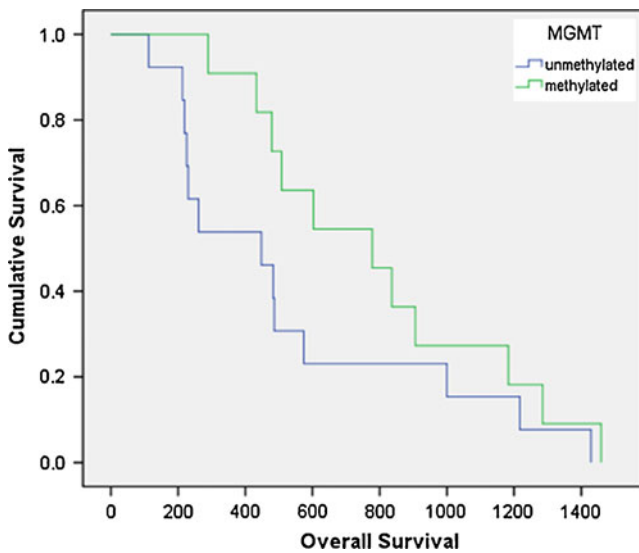
Fig. 1 Kaplan–Meier survival curves for overall survival (OS) in high grade gliomas (HGGs) according the methylation status of MGMT promoter. OS is shown in days

promoter. CT attenuation, similar to the ADC values from DTI, is known to represent the water content of tissue and the tissue cellularity [20, 21]. Considering the fact that the CT attenuation is directly proportional to the electron density of the tissue and the atomic number of the tissue composition in a given volume, the CT attenuation of the tumor is mostly correlated with the tumor cellularity, and it is partly related to the degree of tumor heterogeneity. Unlike homogeneously highly cellular CNS lymphoma with its marked CT hyperattenuation, highly cellular HGGs, which are essentially heterogeneous in texture, tend to be heterogeneous for their CT attenuation as well, although HGGs have shown attenuation as high as that of lymphoma [20]. We speculate that the lower CT attenuation in the MGMT promoter-methylated tumor may suggest, microenvironmentally, a more heterogeneous and/or less cellular texture of the tumor, as compared to that of the MGMT promoter-unmethylated tumor.

Important physiological characteristics of cellular diffusion have been uncovered with the advent of DTI. The ADC indirectly reflects molecular diffusion so that the greater cellular density that inhibits free water movement results in a lower ADC. Hence, the ADC has been regarded as an imaging marker of cellularity for various tumors [22, 23]. Murakami et al. [24] reported that the minimum ADC on pre-treatment MRI is a useful clinical marker for predicting the survival of patients with malignant gliomas. In that study, anaplastic astrocytoma showed higher minimum ADC values than those in GBM. Along with

Fig. 2 Boxplots of the initial CT attenuation (**a**), ADC (**b**), FA (**c**), and rCBV ratio (**d**) of the high grade gliomas according to the MGMT methylation status. The *line across the box* represents the median value. The *box ends* represent the first and third quartiles. The end points of each graph represent the smallest and largest values
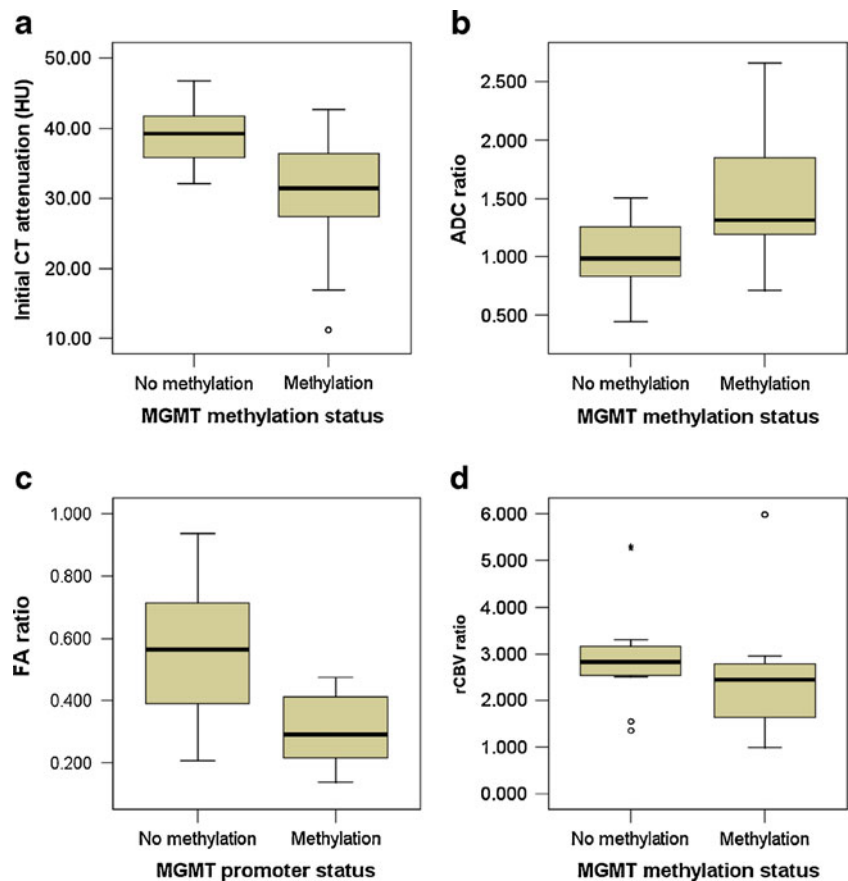
Table 2 Differences of DTI and PWI parameters according to the MGMT promoter methylation status

	No methylation ($n=13$)	Methylation ($n=11$)	p value
ADC	741.52±165.36	1,021.89±375.55	0.055
ADC ratio	1.04±0.32	1.52±0.54	0.032
FA	1,025.57±424.44	552.27±258.67	0.006
FA ratio	0.56±0.22	0.30±0.12	0.007
rCBV ratio	3.02±1.16	2.77±1.70	0.672

the ADC, DTI can provide another parameter called fractional anisotropy (FA). FA is a scalar value ranging from zero to one, and it describes the degree of anisotropy of molecular diffusion. Previous DTI studies on brain tumor suggest that the FA did not differ between low-grade and high-grade gliomas [25]. However, there has been no report on the association of the ADC and FA with the methylation status of the MGMT promoter for HGGs.

In our study, the MGMT-promoter methylated group was likely to have a higher ADC than that of the MGMT-promoter unmethylated group. Considering that in our study population, the MGMT promoter methylation status did not show any difference according to tumor grading or proliferation, the differences of the ADC may mostly depend on the methylation status of the MGMT promoter rather than the tumor grading or proliferation. Perhaps, the tumors with a methylated MGMT promoter may have more heterogeneous or have lower cellularity as compared with the tumors with an unmethylated MGMT promoter, as can be speculated according to the findings of CT attenuation as were discussed above.

Interestingly, significantly lower FA values were observed in the tumors with a methylated MGMT promoter than that in the tumors with an unmethylated MGMT promoter in our study. Previous studies have suggested that the greater destruction of the white matter that occurred due to infiltrative neoplasm, the lower is the fractional anisotropy in the brain tumor [25]. However, the underlying mechanisms for the lower FA in tumors with a methylated MGMT promoter are unknown.

Various MR perfusion methods provide valuable information about tumor angiogenesis and a tumor's capillary permeability, which are important biological markers for tumor grading and the prognosis of gliomas [26, 27]. Among several perfusion parameters, the regional rCBV is the most potent imaging parameter derived from dynamic

susceptibility weighted imaging, and it is a surrogate marker for tumor angiogenesis. Previous studies have reported that the tumor rCBV is strongly correlated with the grade of glioma [28, 29]. A recent study suggested the positive correlation between the tumor rCBV and the VEGF expression for tumors with a WHO grade of II and III [30]. In addition, the rCBV can also help to differentiate therapy-induced necrosis from recurrent tumor by demonstrating different vascularity [14]. In a recent study by Kong et al. [31], the rCBV measured by DSC-PWI immediately after concomitant chemotherapy and radiotherapy for known GBM revealed that the unmethylated MGMT promoter group showed a significant difference of the mean rCBV between the pseudoprogression and tumor progression subgroups, while the methylated group showed no significant difference of the mean CBV between the two subgroups. They suggested that the CBV values were a more powerful predictor of pseudoprogression in unmethylated MGMT promoter group than those values in methylated MGMT promoter group. However, they did not evaluate the difference of the rCBV of the tumors between the methylated MGMT promoter group and the unmethylated MGMT promoter group before treatment.

Our results have revealed no difference of rCBV ratios on preoperative PWI between the methylated and unmethylated MGMT promoter groups. First, the relatively small number of cases may have affected the result. Second, the lack of rCBV ratio difference in our study might be partly due to the fact that we did not correct T1 shortening effect by preload contrast injection or mathematical correction algorithm. Previous study has shown that rCBV corrected for contrast agent extravasation were correlated better with tumor grade of HGGs [32]. Although methylated and unmethylated groups in our study did not differ in terms of tumor grade, there is still a possibility that other factors, such as different degree of angiogenesis and permeability of

Table 3 Difference of imaging features according to the MGMT promoter methylation status

	No methylation ($n=13$)	Methylation ($n=11$)	p value
Ill-defined enhancing tumor margin	1 (7.7%)	5 (45.5%)	0.048
Ring enhancement	10 (76.9%)	7 (63.6%)	0.395
Presence of cyst	0 (0%)	2 (18.2%)	0.199
Heterogeneous T2signal intensity	9 (69.2%)	8 (72.7%)	0.695

Fig. 3 High-grade glioma with a methylated MGMT promoter. **a** Axial non-contrast CT, **b** axial T2WI, **c** axial post-contrast T1WI, **d** ADC map, **e** FA map, **f** rCBV map. Notice that the entire infiltrative enhancing tumor is ill defined with mild peritumoral edema and multiple nodular enhancement (*arrow*), and these are the typical findings of high grade glioma. The pathological diagnosis is glioblastoma (WHO grade IV). The enhancing solid tumor shows variable CT attenuation, ADC, and FA values
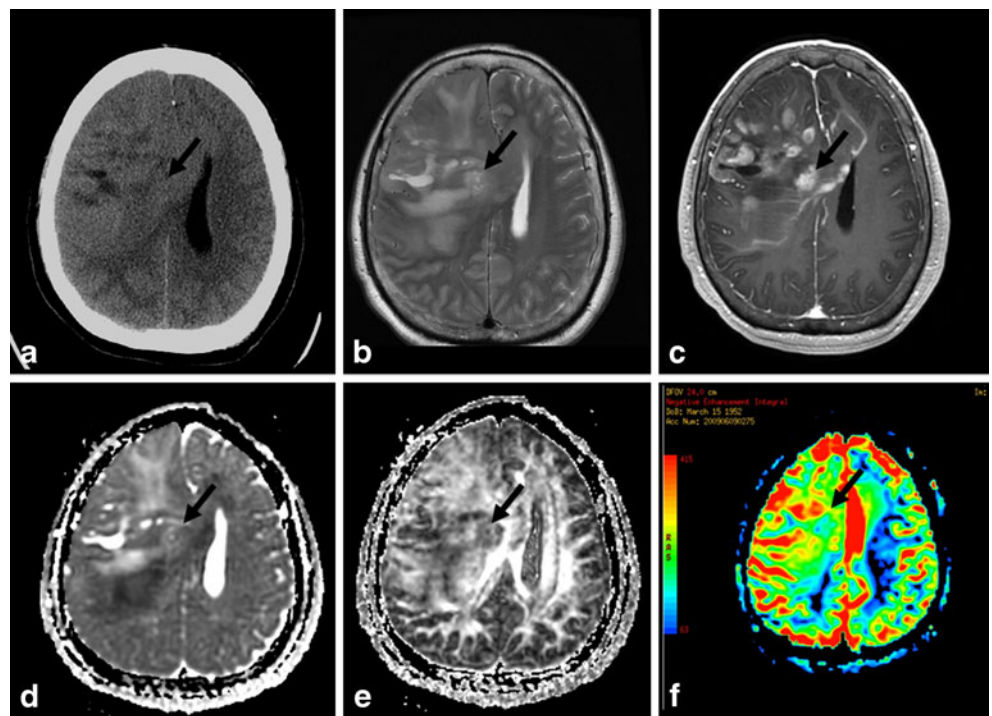

the tumors, can affect the measurement of the rCBV. In a recent study using GBM cell line, MGMT protein was suggested to modulate angiogenesis' of GBM by changing the levels of the different vascular endothelial growth factor receptors [33]. Thus, we can speculate that different rCBV ratio might be expected in respect to the MGMT methylation status of GBM because rCBV is a surrogate marker for angiogenesis. However, our results contradict this speculation. Further study with corrected rCBV map is needed to clarify the true relationship between rCBV and MGMT methylation status.

A recent study reported the relationship between the MR imaging features and the MGMT promoter methylation status [16, 17]. Eoli et al. [17] found that unmethylated tumors were

Fig. 4 High-grade glioma with an unmethylated MGMT promoter. **a** Axial non-contrast CT, **b** axial T2WI, **c** axial post-contrast T1WI, **d** ADC map, **e** FA map, **f** rCBV map. Notice that the enhancing tumor is well defined with moderate peritumoral edema and nodular enhancement. The pathological diagnosis is glioblastoma (WHO grade IV). The enhancing solid tumor (*arrow*) shows a higher CT attenuation, lower ADC, and lower FA as compared to the contralateral white matter
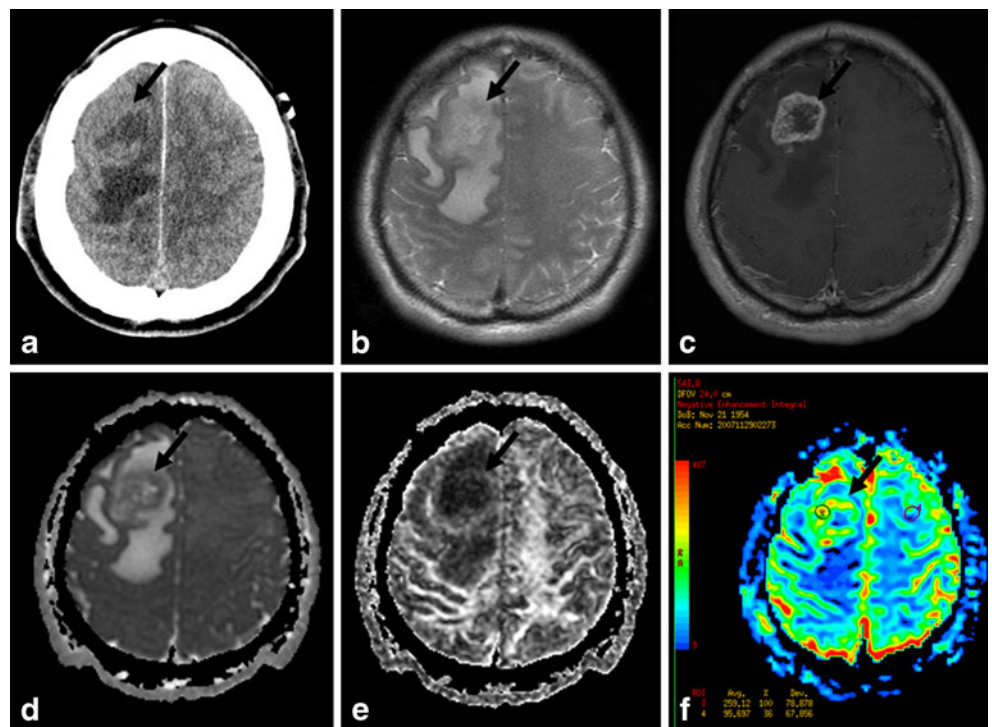
more necrotic and they were more likely to be ring enhancing after contrast injection. Drabycz et al. [16] reported similar findings that ring enhancement is associated with an unmethylated MGMT promoter status (P=0.006). Unlike the two previous studies, we did not find a significant association between ring enhancement and the MGMT promoter methylation status. In contrast to Drabycz's study showing no relationship between an ill-defined enhancing tumor margin and the MGMT promoter methylation status [16], we found that an ill-defined enhancing margin of the tumor was more frequent in the methylated MGMT promoter group than in the unmethylated MGMT promoter group. Perhaps, the differences in the study populations might be the underlying reason for the difference of imaging phenotypes.

There are several limitations to our study. First, the sample size was relatively small, and the study was performed retrospectively. Although all the patients in our study underwent surgery and the lesions were pathologically proven, we did not compare side by side the surgical spacemen and the corresponding imaging. However, majority of our patients underwent near total or gross total resection, and this makes the histological specimen representative of the whole tumor without a significant sampling error. Second, we did not evaluate the postoperative baseline MR images; rather, we evaluated the preoperative MR images for the MGMT promoter methylation status, which is unlike Kong et al. [31]. Our aim was not to evaluate the effect of the MGMT promoter methylation status on pseudoprogression, but instead, we wanted to simply evaluate the relationship between the MGMT promoter methylation status and the preoperative imaging features and the imaging parameters. For predicting the chemosensitivity and the prognosis according to the MGMT promoter methylation status, postoperative baseline MR as well as preoperative MR may be meaningful. Third, we did not use any mathematical correction algorithm or preload contrast injection for PWI so as to remove T1 shortening effect. T1 shortening effect in PWI can erroneously underestimate rCBV especially in case of impairment of blood brain barrier. Fourth, coregistration of the CT and MR images was not performed for the measurement of the CT attenuation values.

Conclusion

This study demonstrates that the MGMT promoter methylation status is associated with a specific imaging feature (an ill-defined margin) and several imaging parameters (lower CT attenuation, a higher ADC, and lower FA) of HGGs. Our results imply that preoperative imaging may predict the MGMT promoter methylation status, which is of paramount importance for predicting the treatment response to chemotherapy with an alkylating agent.

Conflict of interest We declare that we have no conflict of interest.

References

1. Stupp R, Mason WP, van den Bent MJ, Weller M, Fisher B, Taphoorn MJ, Belanger K, Brandes AA, Marosi C, Bogdahn U, Curschmann J, Janzer RC, Ludwin SK, Gorlia T, Allgeier A, Lacombe D, Cairncross JG, Eisenhauer E, Mirimanoff RO (2005) Radiotherapy plus concomitant and adjuvant temozolomide for glioblastoma. N Engl J Med 352(10):987–996
2. Prados MD, Seiferheld W, Sandler HM, Buckner JC, Phillips T, Schultz C, Urtasun R, Davis R, Gutin P, Cascino TL, Greenberg HS, Curran WJ Jr (2004) Phase III randomized study of radiotherapy plus procarbazine, lomustine, and vincristine with or without BUdR for treatment of anaplastic astrocytoma: final report of RTOG 9404. Int J Radiat Oncol Biol Phys 58(4):1147–1152
3. Hegi ME, Diserens AC, Godard S, Dietrich PY, Regli L, Ostermann S, Otten P, Van Melle G, de Tribolet N, Stupp R (2004) Clinical trial substantiates the predictive value of O-6-methylguanine-DNA methyltransferase promoter methylation in glioblastoma patients treated with temozolomide. Clin Cancer Res 10(6):1871–1874
4. Wick W, Hartmann C, Engel C, Stoffels M, Felsberg J, Stockhammer F, Sabel MC, Koeppen S, Ketter R, Meyermann R, Rapp M, Meisner C, Kortmann RD, Pietsch T, Wiestler OD, Ernemann U, Bamberg M, Reifenberger G, von Deimling A, Weller M (2009) NOA-04 randomized phase III trial of sequential radiochemotherapy of anaplastic glioma with procarbazine, lomustine, and vincristine or temozolomide. J Clin Oncol 27(35):5874–5880
5. Weller M, Stupp R, Reifenberger G, Brandes AA, van den Bent MJ, Wick W, Hegi ME (2010) MGMT promoter methylation in malignant gliomas: ready for personalized medicine? Nat Rev Neurol 6(1):39–51
6. Gerson SL (2004) MGMT: its role in cancer aetiology and cancer therapeutics. Nat Rev Cancer 4(4):296–307
7. Hegi ME, Diserens AC, Gorlia T, Hamou MF, de Tribolet N, Weller M, Kros JM, Hainfellner JA, Mason W, Mariani L, Bromberg JE, Hau P, Mirimanoff RO, Cairncross JG, Janzer RC, Stupp R (2005) MGMT gene silencing and benefit from temozolomide in glioblastoma. N Engl J Med 352(10):997–1003
8. Dunn J, Baborie A, Alam F, Joyce K, Moxham M, Sibson R, Crooks D, Husband D, Shenoy A, Brodbelt A, Wong H, Liloglou T, Haylock B, Walker C (2009) Extent of MGMT promoter methylation correlates with outcome in glioblastomas given temozolomide and radiotherapy. Br J Cancer 101(1):124–131
9. van den Bent MJ, Dubbink HJ, Sanson M, van der Lee-Haarloo CR, Hegi M, Jeuken JW, Ibdaih A, Brandes AA, Taphoorn MJ, Frenay M, Lacombe D, Gorlia T, Dinjens WN, Kros JM (2009) MGMT promoter methylation is prognostic but not predictive for outcome to adjuvant PCV chemotherapy in anaplastic oligodendroglial tumors: a report from EORTC Brain Tumor Group Study 26951. J Clin Oncol 27(35):5881–5886
10. Herrlinger U, Rieger J, Koch D, Loeser S, Blaschke B, Kortmann RD, Steinbach JP, Hundsberger T, Wick W, Meyermann R, Tan TC, Sommer C, Bamberg M, Reifenberger G, Weller M (2006) Phase II trial of lomustine plus temozolomide chemotherapy in addition to radiotherapy in newly diagnosed glioblastoma: UKT-03. J Clin Oncol 24(27):4412–4417
11. Prayson RA, Agamanolis DP, Cohen ML, Estes ML, Kleinschmidt-DeMasters BK, Abdul-Karim F, McClure SP, Sebek

BA, Vinay R (2000) Interobserver reproducibility among neuropathologists and surgical pathologists in fibrillary astrocytoma grading. J Neurol Sci 175(1):33–39

12. Coons SW, Johnson PC, Scheithauer BW, Yates AJ, Pearl DK (1997) Improving diagnostic accuracy and interobserver concordance in the classification and grading of primary gliomas. Cancer 79(7):1381–1393

13. Server A, Orheim TE, Graff BA, Josefsen R, Kumar T, Nakstad PH (2011) Diagnostic examination performance by using microvascular leakage, cerebral blood volume, and blood flow derived from 3-T dynamic susceptibility-weighted contrast-enhanced perfusion MR imaging in the differentiation of glioblastoma multiforme and brain metastasis. Neuroradiology 53(5):319–330

14. Cha S (2006) Update on brain tumor imaging: from anatomy to physiology. AJNR Am J Neuroradiol 27(3):475–487

15. Bai X, Zhang Y, Liu Y, Han T, Liu L (2011) Grading of supratentorial astrocytic tumors by using the difference of ADC value. Neuroradiology 53(7):533–539

16. Drabycz S, Roldan G, de Robles P, Adler D, McIntyre JB, Magliocco AM, Cairncross JG, Mitchell JR (2010) An analysis of image texture, tumor location, and MGMT promoter methylation in glioblastoma using magnetic resonance imaging. NeuroImage 49(2):1398–1405

17. Eoli M, Menghi F, Bruzzone MG, De Simone T, Valletta L, Pollo B, Bissola L, Silvani A, Bianchessi D, D'Incerti L, Filippini G, Broggi G, Boiardi A, Finocchiaro G (2007) Methylation of O6-methylguanine DNA methyltransferase and loss of heterozygosity on 19q and/or 17p are overlapping features of secondary glioblastomas with prolonged survival. Clin Cancer Res 13(9):2606–2613

18. Kundel HL, Polansky M (2003) Measurement of observer agreement. Radiology 228(2):303–308

19. Blanc JL, Wager M, Guilhot J, Kusy S, Bataille B, Chantereau T, Lapierre F, Larsen CJ, Karayan-Tapon L (2004) Correlation of clinical features and methylation status of MGMT gene promoter in glioblastomas. J Neurooncol 68(3):275–283

20. Kim DS, Na DG, Kim KH, Kim JH, Kim E, Yun BL, Chang KH (2009) Distinguishing tumefactive demyelinating lesions from glioma or central nervous system lymphoma: added value of unenhanced CT compared with conventional contrast-enhanced MR imaging. Radiology 251(2):467–475

21. von Kummer R, Bourquain H, Bastianello S, Bozzao L, Manelfe C, Meier D, Hacke W (2001) Early prediction of irreversible brain damage after ischemic stroke at CT. Radiology 219(1):95–100

22. Guo AC, Cummings TJ, Dash RC, Provenzale JM (2002) Lymphomas and high-grade astrocytomas: comparison of water diffusibility and histologic characteristics. Radiology 224(1):177–183

23. Squillaci E, Manenti G, Cova M, Di Roma M, Miano R, Palmieri G, Simonetti G (2004) Correlation of diffusion-weighted MR imaging with cellularity of renal tumours. Anticancer Res 24(6):4175–4179

24. Murakami R, Hirai T, Sugahara T, Fukuoka H, Toya R, Nishimura S, Kitajima M, Okuda T, Nakamura H, Oya N, Kuratsu J, Yamashita Y (2009) Grading astrocytic tumors by using apparent diffusion coefficient parameters: superiority of a one- versus two-parameter pilot method. Radiology 251(3):838–845

25. Jellison BJ, Field AS, Medow J, Lazar M, Salamat MS, Alexander AL (2004) Diffusion tensor imaging of cerebral white matter: a pictorial review of physics, fiber tract anatomy, and tumor imaging patterns. AJNR Am J Neuroradiol 25(3):356–369

26. Provenzale JM, Mukundan S, Barboriak DP (2006) Diffusion-weighted and perfusion MR imaging for brain tumor characterization and assessment of treatment response. Radiology 239(3):632–649

27. Barrett T, Brechbiel M, Bernardo M, Choyke PL (2007) MRI of tumor angiogenesis. J Magn Reson Imaging 26(2):235–249

28. Law M, Yang S, Babb JS, Knopp EA, Golfinos JG, Zagzag D, Johnson G (2004) Comparison of cerebral blood volume and vascular permeability from dynamic susceptibility contrast-enhanced perfusion MR imaging with glioma grade. AJNR Am J Neuroradiol 25(5):746–755

29. Emblem KE, Nedregaard B, Nome T, Due-Tonnessen P, Hald JK, Scheie D, Borota OC, Cvancarova M, Bjornerud A (2008) Glioma grading by using histogram analysis of blood volume heterogeneity from MR-derived cerebral blood volume maps. Radiology 247(3):808–817

30. Maia AC Jr, Malheiros SM, da Rocha AJ, Stavale JN, Guimaraes IF, Borges LR, Santos AJ, da Silva CJ, de Melo JG, Lanzoni OP, Gabbai AA, Ferraz FA (2004) Stereotactic biopsy guidance in adults with supratentorial nonenhancing gliomas: role of perfusion-weighted magnetic resonance imaging. J Neurosurg 101(6):970–976

31. Kong DS, Kim ST, Kim EH, Lim DH, Kim WS, Suh YL, Lee JI, Park K, Kim JH, Nam DH (2011) Diagnostic dilemma of pseudoprogression in the treatment of newly diagnosed glioblastomas: the role of assessing relative cerebral blood flow volume and oxygen-6-methylguanine-DNA methyltransferase promoter methylation status. AJNR Am J Neuroradiol 32(2):382–387

32. Boxerman JL, Schmainda KM, Weisskoff RM (2006) Relative cerebral blood volume maps corrected for contrast agent extravasation significantly correlate with glioma tumor grade, whereas uncorrected maps do not. AJNR Am J Neuroradiol 27(4):859–867

33. Chahal M, Xu Y, Lesniak D, Graham K, Famulski K, Christensen JG, Aghi M, Jacques A, Murray D, Sabri S, Abdulkarim B (2010) MGMT modulates glioblastoma angiogenesis and response to the tyrosine kinase inhibitor sunitinib. Neuro Oncol 12(8):822–833